Paper Number:
DOE/MC/31167-97/C0736

Title:
3D Oxide/Oxide Composite Filter

Authors:
J.E. Lane
J-F. LeCostaouec
C.J. Painter
W-F.A. Su
K.C. Radford

Contractor:
Westinghouse Electric Corporation
Science & Technology Center
1310 Beulah Road
Pittsburgh, PA 15235-5098

Contract Number:
DE-AC21-94MC31167

Conference:
Advanced Coal-Fired Power Systems '96 Review Meeting

Conference Location:
Morgantown, West Virginia

Conference Dates:
July 16-18, 1996

Conference Sponsor:
U.S. DOE, Morgantown Energy Technology Center

Disclaimer

3-D Oxide/Oxide Composite Filter

Jay E. Lane (lane.j.e@wec.com, 412-256-2195)
Westinghouse Electric Corporation
Science & Technology Center
1310 Beulah Road
Pittsburgh, PA 15235-5098

Jean-Francois LeCostaouec (603-335-2115)
Techniweave, Inc.
109 Chestnut Hill Road
Rochester, NH 03868

Carol J. Painter[1] (412-256-2202)
Wei-Fang A. Su[1] (412-256-2096)
Ken C. Radford[1] (412-256-1266)
Northrop Grumman Corporation
1310 Beulah Road
Pittsburgh, PA 15235-5098

Introduction

Hot gas particulate filters are key components for the successful commercialization of advanced coal-based power-generation systems such as Pressurized Fluidized-bed Combustion (PFBC), including second-generation PFBC, and Integrated Gasification Combined Cycles (IGCC). Current generation monolithic ceramic filters are subject to catastrophic failure because they have very low resistance to crack propagation. To overcome this problem, a damage-tolerant ceramic filter element is needed.

Objectives

Westinghouse, with Techniweave as a major subcontractor, is conducting a three-phase program aimed at providing advanced candle filters for a 1996 pilot scale demonstration in one of the two hot gas filter systems at Southern Company Service's Wilsonville PSD Facility. The Base Program (Phases I and II) objective is to develop and demonstrate the suitability of the Westinghouse/Techniweave next generation composite candle filter for use PFBC and/or IGCC power generation systems. The Optional Task (Phase III, Task 5) objective is to fabricate, inspect and ship to Wilsonville 50 advanced candle filters for pilot scale testing.

---

[1]Formerly of Westinghouse Electric Corporation

Research sponsored by the U.S. Department of Energy's Morgantown Energy Technology Center, under contract DE-AC21-94MC31167 with Westinghouse Electric Corporation, Science & Technology Center, 1310 Beulah Road, Pittsburgh, PA 15235-5098; FAX (412) 256-1267.

A major objective of the base program is to develop an oxide CMC (ceramic matrix composite) candle filter that is cost competitive with prototype next generation filters. This goal is to be achieved through the use of a low cost sol-gel fabrication process and a 3D fiber architecture optimized for high volume filter manufacturing. During the Base Program, manufacturability for large scale filter production will be assessed in order to meet the needs of commercial scale power generation facilities. The results from this assessment will be implemented during the Optional Task.

Approach

This project plans to develop an advanced filter with damage tolerance, increased durability, increased resistance to crack propagation, and non-catastrophic metal-like failure characteristics through the use of:

- A 3D continuous fiber preform for reinforcement;
- Oxide materials, which are inherently stable in oxidizing environments and have been shown by Westinghouse under DOE Contract #DE-AC21-88MC25034, Thermal/Chemical Degradation of Ceramic Cross-Flow Filter Materials, to be more resistant to corrosive alkali species than nonoxides, such as SiC and Si_3N_4; and,
- Low cost sol-gel processing.

Project Description

Westinghouse and Techniweave have undertaken a three-phase program to develop an advanced ceramic composite oxide-based. Recently completed, Phase I, Filter Material Development and Evaluation, activities included the laboratory-scale development, characterization, and testing of a mullite matrix 3D fiber-reinforced (Nextel 550) ceramic composite filter material. This effort focused on developing the base filter material, minimizing fabrication costs and meeting filter material requirements.

Currently ongoing, Phase II, Prototype Filter Fabrication and Evaluation, activities include additional coupon testing of Nextel 610 (polycrystalline alumina fiber) and Nextel 720 (polycrystalline alumina + mullite fiber) CMC filter materials, the development of a prototype filter, and filter qualification testing in a simulated pressurized-bed combustion environment in the Westinghouse High-Temperature High-Pressure (HTHP) filter test facility.

Phase III, Optional Pilot-Scale Filter Manufacturing, activities include the manufacture of 50 full size candle filters for pilot scale testing at Wilsonville and implementation of quality assurance/quality control and non-destructive evaluation procedures developed in Phase II.

A breakdown of the experimental activity for the recently completed Phase I, Task 3 (Tasks 1 and 2 were the NEPA Report and Test Plan, respectively) and for the ongoing Phase II, remainder of Task 3 and Task 4, follows:

Phase I

Task 3 - Development, Qualification, and Testing of Hot Gas Filter
- 3.1 - Coupon Development, Fabrication, and Testing
  - 3.1.1 - Develop 3D Fiber Architecture
  - 3.1.2 - Develop Composite Filter Material Fabrication Process
  - 3.1.3 - Fabricate and Evaluate Best Filter Material

Phase II

Task 3 - Development, Qualification, and Testing of Hot Gas Filter
- 3.1 - Coupon Development, Fabrication, and Testing
  - 3.1.3 - Fabricate and Evaluate Best Filter Material
- 3.2 - Develop and Evaluate Prototype Candle Filters
  - 3.2.1 - Weave Filter Preforms
  - 3.2.2 - Make Prototype Candle Filters and Tubes
  - 3.2.3 - Evaluate Prototype Filters

Task 4 - Manufacturing of Hot Gas Filter
- 4.1 - Filter Manufacturing Plans
- 4.2 - Filter Materials Test Plan
- 4.3 - Topical Report

Results

To date, Phase I has been completed. Phase I activities included laboratory-scale development, characterization, and testing of a mullite matrix 3D fiber-reinforced (Nextel 550) ceramic composite filter material. Nine 3D architectures were designed, preforms and CMCs made, tested and evaluated. Permeability, 4-pt bend strength, and microstructural evaluation results were used to downselect to one 3D architecture. High-temperature flow-through corrosion tests up to 400 h and thermal aging tests in static air up to 5000 h were conducted. Based on the above testing, two improvements were made to the filter material. First, modifications were made to the fiber architecture to increase the maximum breaking load. Second, Nextel 550 fiber will be replaced with Nextel 610 or 720 in order to increase corrosion resistance. Additionally, composite test panels made with N610 and N720 showed a significant increase in room temperature bend strength as compared to N550 filter material CMCs. These results are presented in more detail in the remainder of this paper.

3D Fiber Architecture Development

A low cost, three-dimensional (3D) fiber architecture, that is both easy-to-manufacture and automatable, is required to produce an economical 3D preform suitable for candle filter use. Toughness in all directions, good shear properties, homogeneously distributed porosity, and surface smoothness are desirable features for selecting a preform for fabricating a ceramic matrix composite (CMC) candle filter fiber preform. A 3D fiber architecture can be designed to fulfill these requirements. Techniweave's fiber architecture design philosophy has been guided by the selection of automatic net shape weaving techniques, the generation of thin wall

structures, the achievement of fiber continuity through highly stressed regions and the tailoring of the preform to the mode of matrix introduction.

Over the past five years, Techniweave has developed equipment and process technology for weaving seamless, tubular filter preforms with ceramic fibers. During an IRAD program, the use of a multilayer fabric was demonstrated for fabricating a porous mullite/mullite CMC. This technology provides the basis for the fiber architecture variations being evaluated in this program for the economical production of a fiber preform for candle filters. A generic sketch of the multi-layer fabric is presented in Figure 1.

From this baseline weave, Fig. 1, nine fiber architectures were designed to examine the effect of fiber volume, wall thickness, fiber architecture and yarn construction on the CMC filtration characteristics and mechanical properties. The fiber orientation and yarn construction were varied to modify the sizes and distributions of porosity in the preform. The amount of fiber at the preform surface was varied to control the filtering surface smoothness and porosity.

In order to downselect to the best architecture, ceramic composites were fabricated, using the process shown in Figure 2, from each of the nine architectures. Each composite was evaluated for permeability, room temperature 4-point bend strength, toughness, weaving feasibility and potential manufacturing cost. Permeability was measured with a 41 mm diameter disc sample in the Westinghouse permeability rig. Acceptable permeability results from this test rig are gas flow resistance values < 1 in-wg/fpm at room temperature. Bend strength test specimens, 6 mm x 45 mm were machined from both the warp and fill directions of the composite plates and tested according to ASTM C1161-90. The warp and fill directions correspond to the axial and circumferential, or hoop, directions, respectively, of the candle filter geometry. Toughness was determined by a qualitative examination of the load-deflection curves. Weaving feasiblity was evaluated by weaving a closed end section of a filter tube.

The typical macrostructure of the ceramic composite filter materials is shown in Figure 3. The filtering surface has an in-situ deposited membrane layer. As can be seen in the figure, the matrix concentration decreases through the thickness from the dirty gas side to the clean

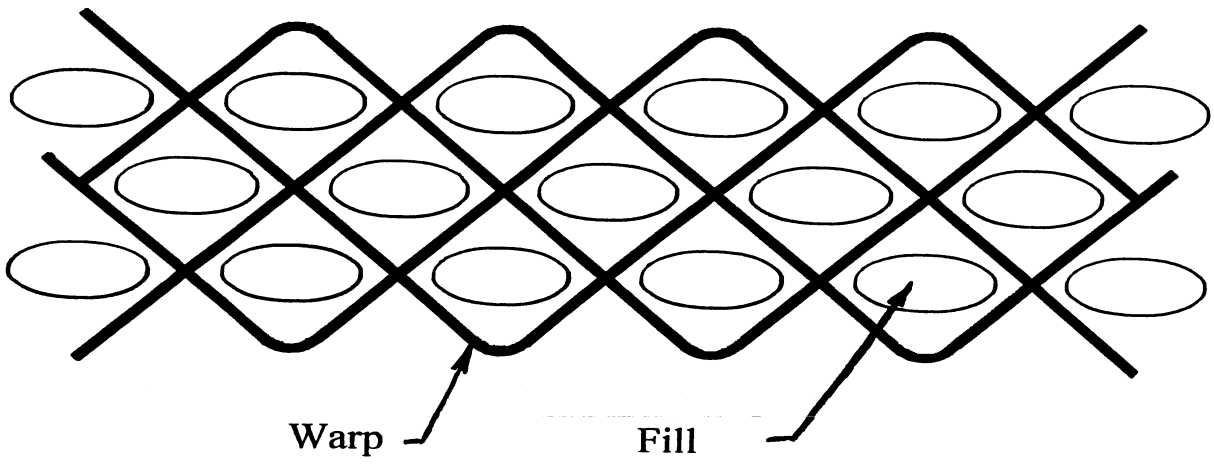

Figure 1. Schematic of multi-layer fabric where the warp yarns provide axial and radial reinforcement while fill yarns provide hoop reinforcement.

gas side. The typical bulk density range for these composites was 1.17 to 1.44 g/cm^3.

Permeability. Gas flow resistance, or permeability, values for all architectures met the gas flow resistance requirement of < 1 in-wg/fpm at room temperature. Permeability was not able to be used as a discriminator in the architecture downselect process.

Mechanical Properties. The downselect process quickly narrowed in on strength and toughness as the primary discriminators between the various architectures. Permeability and cost of fabrication were non-issues as all architectures met the permeability requirements and initial preform weaving trials showed that fabrication costs were expected to be similar. The remainder of this discussion focuses on the differences in strength and toughness as related to the different architectures. The effects of fiber volume, fiber architecture, and matrix content on strength are discussed as is a qualitative analysis of toughness. Table 1 shows the relevant data for this discussion.

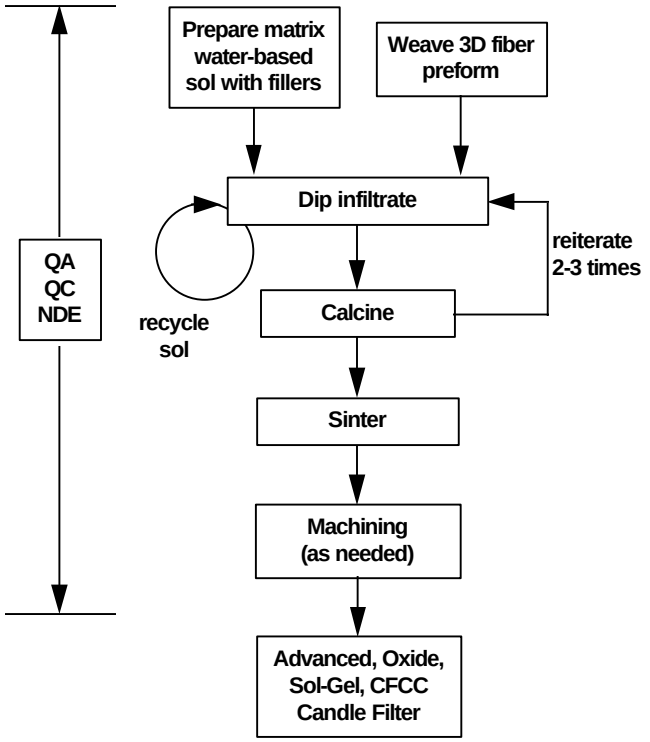

Figure 2 Filter Material Fabrication Process

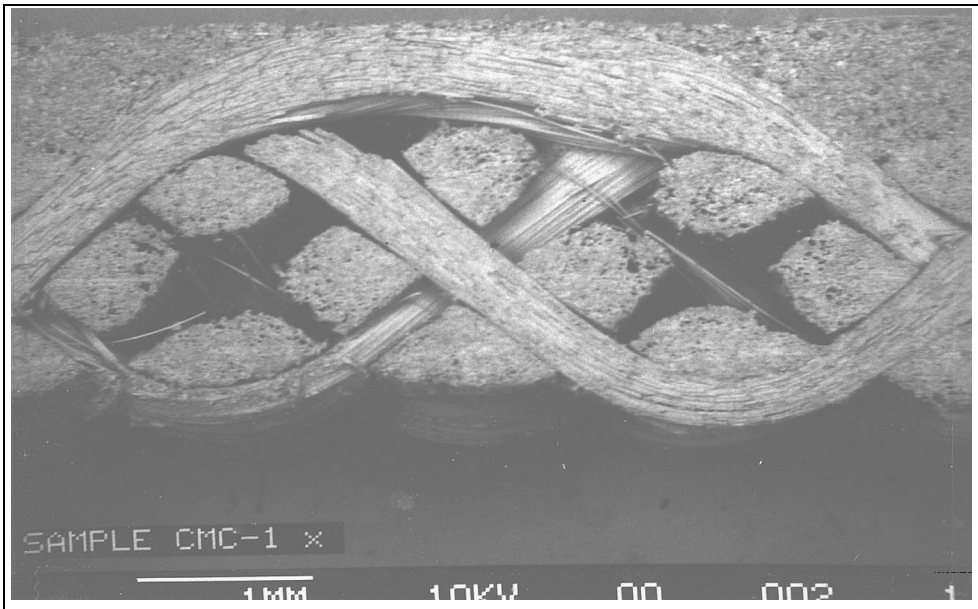

Figure 3 Cross-Sectional View of a Typical Composite Filter Material

Table 1 -- Room Temperature 4-Point Bend Strength Results

CANDIDATE ARCHITECTURES		PREFORM DATA				CMC	CMC BEND STRENGTH	
		Thick.	V_{fw}	V_{ff}	Vf_{tot}	Density	Warp Dir.	Fill Dir.
No.	Description	in.	%	%	%	g/cm³	(psi	(psi)
1	3 surface float	0.080	18	15	33	1.40	1058 ± 224 (5)	1577 ± 455 (6)
2	2 surface float	0.080	17	17	35	1.43	1100 ± 80 (5)	1731 ± 214 (6)
3	2 surface float random	0.080	17	17	34	1.42	1322 ± 289 (5)	1931 ± 328 (5)
4	2 surface float random	0.065	21	12	33	1.25	1104 ± 119 (6)	917 ± 429 (6)
5	baseline warp interlock	0.069	~13	~19	32	1.39	1888 ± 367 (6)	921 ± 122 (6)
6	2 surface float fugitive yarn random	0.064	~14	~11	25	1.79	2076 ± 563 (6)	2061 ± 973 (6)
7	2 surface float random	.0970	19	10	29	1.18	843 ± 255 (12)	625 ± 148 (6)
8	2 surface float random	.0920	16	12	28	1.68	929 ± 148 (10)	1427 ± 328 (6)
9	2 surface float random	.070	20	8	28	1.36	2144 ± 522 (10)	1201 ± 522 (9)

V_{fw}: fiber volume in warp direction; V_{ff}: fiber volume in fill direction; VF_{tot}: total fiber volume
value in parentheses represents number of specimens tested

Effect of Fiber Volume on Strength.

The nine architectures were woven into preforms with total fiber volume ranging from 25 to 35%. Fiber volume in the warp and fill directions was normalized to compare the various architectures. Preforms 5 and 6 were excluded from this analysis as insufficient material was available to accurately measure the fiber volume in the fill (circumferential direction of a filter) and warp (axial or along the length of a filter) directions.

The fiber volume in the fill direction consists of straight fiber tows completely aligned in what would be the circumferential direction of a candle filter. Thus, 100% of the fill fibers are contributing to the strength in the fill direction.

In contrast, the fiber volume in the warp direction, although running in the axial direction of a filter, is not straight but is interwoven around the fill fibers. Thus, the warp fibers have a large proportion of the fiber going through the preform thickness and a lesser quantity of fiber directly aligned in the warp or axial direction. The warp fiber strength is divided to give through thickness strength and integrity to the preform and to give axial strength along the candle filter.

The length of the float (fibers running parallel to the surface in the warp direction) directly contributes to the axial reinforcement with the basic angle interlock architecture #5, which has no fiber parallel at the surface, and the three surface float architecture #1, most fiber parallel at the surface, being the two extremes. The contribution of the warp fibers to the axial reinforcement is, however, more directly dependent on the preform thickness. Thinner wall architectures exhibit through thickness fibers having a smaller angle with the axial direction (i.e., the degree of misalignment with the axial direction is smaller with thinner preforms than thicker ones) which increases their contribution to strength in the axial direction.

Fill Direction Effects. A direct correlation could not be established between strength and the amount of fiber volume in the fill direction. However, composites with fiber volume

greater than 15% in the fill direction, #1, #2, and #3, exhibited greater strength than those with 8-12 % fiber volume.

Examination of the ultimate strength for candidates #4, #7, #8, and #9 indicate that other factors besides fiber volume contribute to the composite strength. Comparison of the #4 to #9 and #8 to #9 would suggest that composite density is also affecting strength, see Table 1. The density of the composite is strongly related to the amount of mullite matrix (from sol + filler powder) in the preform. The penetration of the mullite powder within the preform is affected by the preform architecture (geometrical thickness and yarn construction, or the yarn denier and twist) and the degree of repeatability of the infiltration process.

Warp Direction Effects. Direct comparison of the composite mechanical strength in the warp direction for the different CMCs was only conducted for preforms with equivalent thickness (see prior discussion on fiber volume effects). This comparison was further narrowed to the preforms exhibiting the same double float architecture with the random design: #3, #4, #7, #8, and #9. Normalized fiber volume in the warp direction varied between 16 - 20%. Preform thickness ranged from 0.064 in. to 0.097 in. Given the above constraints, only two sets of architectures were available for direct comparison: #7 to #8 and #4 to #9.

The lowest strengths in the warp direction are observed for #'s 7 and 8, which have thicker preforms, 0.097 in. and 0.092 in., respectively, and intermediate fiber volumes, 18% and 16%, respectively. The strength of these two composites, 843 psi and 929 psi, respectively, is essentially the same.

The other two composites exhibiting similar thickness are #4 and #9, 0.065 in. and 0.070 in., respectively. The normalized warp fiber volume is the same for both composites, about 20%. Analysis of the strength results is complicated because for #4 changes in bend specimen width affected the magnitude of the bend strength; wider specimens were stronger than narrow specimens. The narrow specimen data is given less weight in this analysis because the wider specimens provide a more uniform and representative cross-section of this architecture for bend testing. Composite #9 was tested using wider specimens. The strengths of #4 and #9 are 1908 and 2144, respectively. These strengths are comparative and could be considered relatively the same given the wide standard variations associated with these samples.

The partial conclusions from the review of data in the fill direction were:

- It is possible to achieve reasonable strength level (1200 psi) with only a small amount of fiber in the fill direction (8%).
- Higher strength level (up to 2300 psi) can be achieved with 15% fiber volume.
- The amount of matrix affects the strength level. The respective contributions of the fiber and matrix to the composite strength are not known and their determination is not a trivial issue.

The partial conclusions for the warp direction were:

- Width of the flexure bar specimens can affect the strength data. It is recommended that all future testing be conducted with specimens at least 6 mm (0.24 in.) in width.
- An average bend strength of 2100 psi in the warp direction can be achieved with double float architectures which have low fiber volumes (~11% for #6) and high

densities (1.79 g/cc) or matrix content and which have high fiber volumes (20% for #9) and lower densities (1.36 g/cc) or less matrix content.

Effect of Fiber Architecture on Strength.

Recognizing the complexities in interpreting the test results (limited characterization, sample size effects, etc.) two items, length of the surface float and design repetition, related to the preform architecture were however isolated and are discussed below.

Effect of the Length of Surface Float. Comparison of #1 (3 surface float) and #2 (2 surface float) indicated that the two surface float architecture design provided a narrower spread of strength values than does the three surface float design. The three float design was examined in an attempt to achieve a smoother surface. This approach however does not provide as rigid a preform as does the two surface float. Thus, additional manipulation of the surface float preform would cause variations in the preform which would result in composites with widely varying properties. As noted previously, the use of stuffers in this case would be expected to greatly increase the stability of the preform and result in composite filter materials with more uniform and repeatable properties.

Effect of Design Repetition. Composites #2 and #3 were prepared from preforms exhibiting similar characteristics except for the repetitiveness of the pattern. The #2 architecture has a more oriented fiber pattern than does #3. This preferred orientation of #2 resulted in a rougher surface with aligned ridges and valleys. The random pattern of #3 showed a more uniform surface. Providing a random orientation of the pattern seems to also have a beneficial effect on the mechanical properties of the material; a smoother more uniform surface has less stress concentrations than would the surface of #2. The strength of #3 was slightly higher than that of #2.

Effect of Matrix on Composite Strength.

Architecture #6 was designed with a fugitive yarn to yield a more open composite for improved permeability characteristics. The composite made from #6 had a low fiber volume and a high strength in both directions. The high strength was due to the high density which resulted from a large amount of matrix in the composite. This composite had more matrix because of the fugitive fiber which provided additional surface area to deposit the matrix on during infiltration processing. However, toughness, as discussed below, must also be considered when choosing the right amount of matrix and fiber.

Qualitative Evaluation of Toughness

An appropriate test for toughness is difficult to determine for these composites due to their low thickness. The approach taken here was to compare the shapes of the load-deflection curves (deflection was measured during bend testing with a three probe extensometer) for the various architectures (Note, the load-deflection curves are not shown here because they did not scan very well, but copies of the curves are available for evaluation by contacting the program manager).

A material exhibiting a higher strength at the point where the composite loses linearity, i.e. “yields”, (defined in dense composites as the first micro-cracking stress/load) and showing a significant load carrying ability beyond that point can intuitively be qualified as a tougher composite. This point in essence also takes into account the area under the curve. Using this

criteria, #4 (warp direction data only available) was considered the least suitable and #9 was considered the most desirable architecture. Composite #9 exhibits a “yield stress” of 1280 psi in the warp direction and subsequently carried a load to a 2100 psi level and continued to exhibit good strain carrying capability beyond the ultimate load point thus demonstrating a noncatastrophic failure mode.

Architecture Downselect

The architecture downselect process picked #9. The downselect was conducted by direction as follows:

Warp.

- The axial (warp) direction of the candle filter is subjected to bending loads. Candidates with warp strengths less than 1000 psi were first rejected -- #7 and #8.
- Architectures with a nonrandom (oriented design) were rejected (for reasons discussed previously). This left architectures #3, #4, #5, #6, and #9.
- The composites exhibiting the highest warp strengths were then selected. These were #3, #6 and #9.
- Toughness then was considered and #9 had the best qualitatively determined toughness. Architecture #3 might have been further considered if there was additional strength data with wider bend bar specimens for evaluation. Architecture #6 did not have load-deflection data for the warp direction. However, a #6P, the P represents the use of pressure during matrix processing, did have load-deflection curves. From these curves, is was determined that #6 had a low degree of toughness, most likely due to its high matrix content which made it act more like a monolithic.

Fill.

- Using the first two criteria above, minimum strength and randomness of design, the list was narrowed to #3, #6, #8, and #9.
- In general, load-deflection curves in the fill direction showed less load carrying ability after the initial “yield” than those of the warp direction. Again, #6 exhibited poor toughness. This left #3, #8 and #9.
- Combining the results above, #8 was rejected due to its low warp strength. Given the available data, #9 was chosen over #3 due to its higher warp strength and because it had the best toughness characteristics.

In summary, fiber architecture #9, a random double float architecture, was selected because adequate flexure strength was obtained in both the warp and fill directions and because the load-deflection curves exhibited the best toughness.

CMC Evaluations

Two types of tests were conducted to determine the effects of temperature, time, and the environment on the Nextel 550-based filter composite material’s mechanical properties and failure characteristics. First thermal aging tests were conducted in which bend specimens were exposed to 150, 300, 800, 2000, and 5000 h at 870°C in static air and then bend tested at

room temperature. Because there was insufficient material from any one architecture to conduct these tests, specimens were used from the first six architectures for the thermal aging experiments. These specimens all had the same matrix composition and were processed identically. The resulting thermal aging bend data was then normalized with respect to the as-received bend data in order to eliminate architecture effects.

Second, four high-temperature, flow-through corrosion tests were conducted in which specimens were exposed to of 400 h at 870°C with simulated pulse cycling in flow-through steam/air with and without alkali. Post-test characterization included high temperature bend testing and microstructural evaluation.

Thermal Aging

Figure 4, shows the normalized bend strength vs. exposure time. From this data, up to 5000 h in static air at 870°C, there appears to be little effect of temperature on strength. Consequently, x-ray diffraction was conducted for each of the thermally aged specimens. X-ray diffraction (XRD) data did not show any change in phase chemistry of the samples. The XRD spectrum for the 5000 h data can be directly overlaid on the 2000 h spectrum and the as-received (unaged) spectrum without any noticeable differences in any of these spectra. (Note, the x-ray diffraction curves are not shown here because they did not scan very well, but copies of the curves are available for evaluation by contacting the program manager).

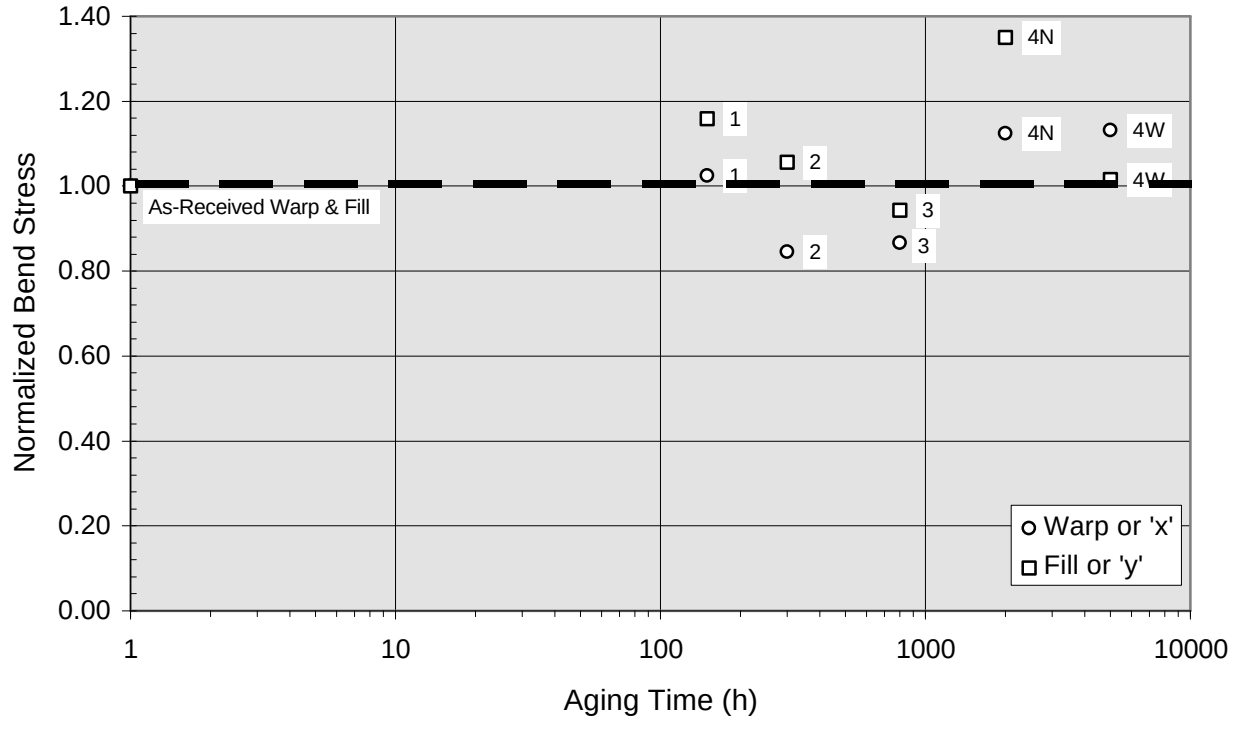

Figure 4 Effect of Thermal Aging at 870°C in Static Air on Room Temperature 4-pt Bend Strength

High Temperature Flow Through Corrosion Testing

Figure 5(a) and (b) clearly demonstrate the results of the flow through corrosion testing. Discs, Fig. 5(a), exposed to steam/air only survived the tested, whereas, discs, Fig. 5(b), exposed to steam/air containing 20 ppm sodium cracked longitudinally in the center, where the stresses would be the highest during backpulsing. Subsequent SEM examinations of the sodium exposed samples showed crystallization along the outer surface of the Nextel 550 fibers. EDAX, energy dispersive x-ray, analyses of these same regions showed the presence of sodium and silicon with a lower concentration of aluminum than expected.

These high-temperature, flow-through tests conducted with Nextel 550 reinforced ceramic composite filter materials showed that this material was susceptible to alkali (Na) attack. The as-produced Nextel 550 fiber is composed of δ- and γ-alumina and amorphous silica. SEM and EDAX analyses indicated that the Nextel 550 fiber, with this amorphous silica phase, was probably attacked by the sodium resulting in devitrification of the amorphous silica which caused embrittlement of the fiber. The test coupons used for the high temperature steam/air/alkali test (870°C, 400 h) broke in two either during testing or immediately upon removal from the test rig; these coupons were highly embrittled. The test coupons subject to steam/air-only were not embrittled and were intact, and remained intact, after removal from the test rig.

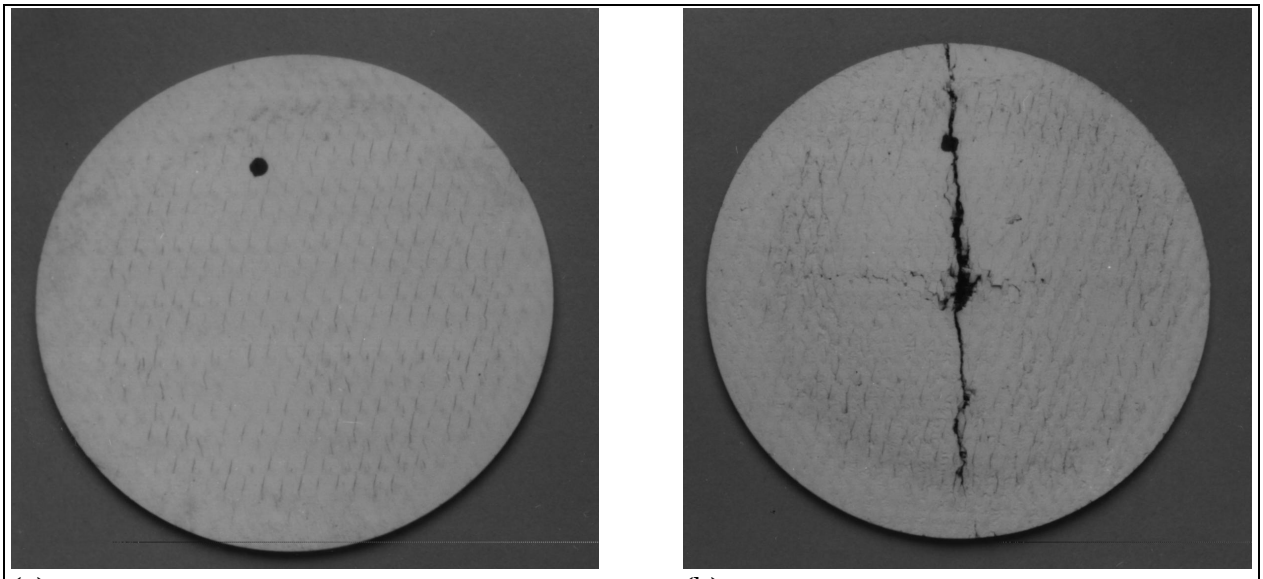

(a) (b)

Figure 5 Optical photographs of flow through test specimens exposed to 870°C for 400 h in (a) 5-7% steam and (b) 20 ppm NaCl/5-7% steam/air

Filter Material Improvements

Bend strength testing and the high temperature, flow-through testing raised the following two technical issues. These issues are discussed in the following paragraphs and the approaches to resolve them are discussed in the following subsections.

First, the ultimate breaking loads, < l lb (see Table 1), were considered to be too low, even though the material had sufficient strength, 1000-2000 psi, for filter use. These low breaking loads were primarily due to thin wall structures, 0.100 in., and low fiber volume fractions, < 30 %. Thin wall preforms and minimized fiber volumes were targeted in order to reduce cost. Although, the breaking loads are low for the coupon samples, it is unclear whether or not this would be an issue for full size candle filters. Potential filters made from this material were considered to be susceptible to breakage during handling and installation.

Second, the filter composite material was embrittled during flow-through testing in an alkali environment as discussed in the previous section. Although this test is relatively harsh, it may be considered an accelerated environmental test which could be indicative of long-term material behavior. The embrittlement was due to devitrification of the amorphous phase in the fiber Nextel 550 fiber.

Architecture Modifications

The downselected architecture #9 was modified by adding stuffer yarns which increased the preform thickness. This modification not only raised the breaking load capability of the filter material, as shown in Table 2, but also increased the filter composite material strength as shown in the table. Stuffer architectures #10-#13 represent different combinations of stuffer fiber amount, direction(s) of stuffer fiber, and preform wall thickness. The highest breaking load, warp - 6.6 lb and fill 8.2 lb, was achieved by CMC 13 with a 0.15 in. wall thickness. However, this architecture also uses the most fiber and would result in the highest cost filter of the four stuffer architectures shown in the table.

Architectures 11 and 12 had lower fiber volumes, comparable to the downselected conventional architecture 9, would have comparable filter fabrication costs, and do provide an increased breaking load. These architectures also provide significant strength benefits, without sacrificing cost by increasing fiber volume, as a result of the stuffer modifications the preform architecture, see Figure 6. Based on a qualitative evaluation of the load-deflection curves, toughness for the stuffer modified composites appeared to be better than for architecture 9.

Table 2. Summary of Mechanical Testing Results for CMC 9 and Stuffer Modified CMCs 10-13

Sample ID	Mean Thick (in.)	Warp Direction (X)		Fill Direction (Y)	
		Mean Strength* (psi)	Breaking Load (lb)	Mean Strength* (psi)	Breaking Load (lb)
9 conventional	0.059	2144 ± 522 (10)	0.64	1201 ± 522 (9)	0.45
10	0.073	3731 ± 160 (4)	3.0	1652 ± 223 (5)	1.6
11	0.069	3745 ± 284 (5)	2.8	2525 ± 245 (3)	2.1
12	0.105	3745 ± 165 (4)	3.3	3044 ± 300 (4)	6.2
13	0.149	2334 ± 280 (5)	6.4	1958 ± 440 (5)	8.2

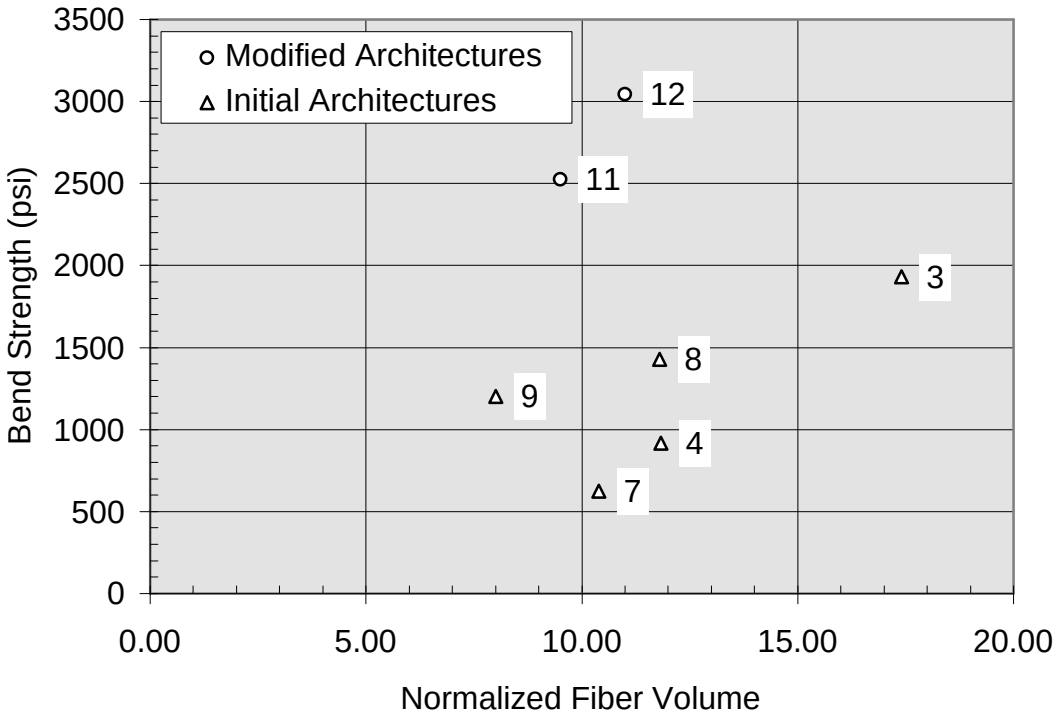

Figure 6 Plot of bend strength vs normalized fiber volume which show the effects of architecture and fiber volume on strength.

*number of samples tested is shown in parentheses

Reinforcement Fiber Selection

Nextel 610 (alumina) and Nextel 720 (polycrystalline mullite+alumina) were evaluated as replacements for the Nextel 550 fiber. Preforms were woven using an architecture similar to the stuffer modified architectures 11 and 12. For the Nextel 610 fiber, the precrystallized version was used to weave the preforms. Due to its lower elastic modulus, i.e., reduced stiffness, precrystallized N610 is much easier to weave than crystallized N610. After weaving the precrystallized N610 preform is subjected to a heat treatment cycle which converts the fiber to normal fully crystalline N610. Both preforms were fabricated with stuffers and double floats, based on prior fiber architecture development work discussed earlier. The stuffers increase the breaking load capability and the double floats provide a smoother surface more applicable for ash cleaning during backpulsing. Table 3 provides the relevant measured characteristics of the two preforms.

The preforms were processed in the same manner as the architecture 9 and stuffer modified architectures. Bend bars were machined from each specimen and tested at room temperature. The preform architecture used for both the N610 and N720 samples is most similar to N550 (N550) architectures 11 and 12, which are stuffer modified versions of architecture 9.

Table 3 -- Characteristics of N720 and N610 3D Fiber Preforms

Characteristic	Preform 15	Preform 16
Fiber Type	N720 alumina+mullite	N610 alumina
Thickness (in.)	0.120	0.120
Fiber Volume (%)	30	26.5
Fill (%)	13.9	11.5
Warp Stuffer (%)	6.8	6.0
Warp Interlock (%)	9.3	9.0

Table 4 compares the mean strength and breaking load results of Nextel 550 CMCs 9 and 10-13 (stuffer-modified) to that of Nextel 610 CMC 16-3 and Nextel 720 CMCs 15-3 (warp, or candle axial, direction) and 15-4 (fill, or candle circumferential, direction). These CMCs were all processed using the same standard baseline Techniweave process. The N610 CMCs, in the fill direction, are 42% stronger and have a 42% higher breaking load than the best N550 CMC in the table.

The N720 CMCs are 50% and 94% stronger in the warp and fill directions, respectively, than the best N550 CMCs shown. The greatest improvement is in the breaking load which for the N720 CMCs is 165% and 152% stronger in the warp and fill directions, respectively, than the best N550 CMC shown. Because of the improved breaking loads, the use of either the N610 or N720 fiber greatly increases the handleability of this filter material. Qualitatively both materials also exhibited improved toughness over the Nextel 550 CMCs.

Table 4 -- Bend Strength and Breaking Load Comparison of Filter CMCs made with Nextel 550, 720 and 610 Fibers (All CMCs were processed the same and fired at the standard baseline processing temperature)

Sample ID	Warp Direction (X)		Fill Direction (Y)	
	Mean Strength* (psi)	Breaking Load (lb)	Mean Strength* (psi)	Breaking Load (lb)
Nextel 550 CMCs				
9 - conventional	2144 ± 522 (10)	0.64	1201 ± 522 (9)	0.45
10 - stuffer	3731 ± 160 (4)	3.0	1652 ± 223 (5)	1.6
11 - stuffer	3745 ± 284 (5)	2.8	2525 ± 245 (3)	2.1
12 - stuffer	3745 ± 165 (4)	3.3	3044 ± 300 (4)	6.2
13 - stuffer	2334 ± 280 (5)	6.4	1958 ± 440 (5)	8.2
Nextel 720 CMCs with preform architecture similar to 11 & 12				
15-3 (warp) and 15-4 (fill)	5507 ± 408 (3)	17.0	5910 ± 628 (3)	20.7
Nextel 610 CMCs with preform architecture similar to 11 & 12				
16-3	not measured	not measured	4334 ± 1168 (3)	11.69

*number of samples tested is shown in parentheses

Future Activities

Future, Phase II, activities consist of conducting high temperature flow-through corrosion tests and short-term (~600 h) thermal aging tests of the above discussed Nextel 610 and Nextel 720 based composite filter materials. The test results will be used to select a fiber to be used for fabricating 1.0 m long candle filters which will be subjected to a series of tests in the Westinghouse High Temperature, High Pressure Filter Test Facility.

Acknowledgments

The authors wish to acknowledge the program support and technical guidance provided by Ted McMahon, the METC/COR, over the course of Phase I, 9/30/94 - 5/31/96. We would also like to thank Mary Ann Alvin for her technical suggestions, the permeability analyses, and with Rich Kunkle, the conduct of the high temperature flow through corrosion tests; Mike Biondi for his diligent work in the laboratory; Tom Mullin for the SEM support; and, Paula Freyer for the XRD analyses.